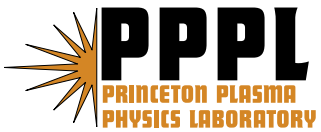

Princeton Plasma Physics Laboratory

PPPL-

PPPL-



Prepared for the U.S. Department of Energy under Contract DE-AC02-09CH11466.

Princeton Plasma Physics Laboratory

Report Disclaimers

Full Legal Disclaimer

This report was prepared as an account of work sponsored by an agency of the United States Government. Neither the United States Government nor any agency thereof, nor any of their employees, nor any of their contractors, subcontractors or their employees, makes any warranty, express or implied, or assumes any legal liability or responsibility for the accuracy, completeness, or any third party's use or the results of such use of any information, apparatus, product, or process disclosed, or represents that its use would not infringe privately owned rights. Reference herein to any specific commercial product, process, or service by trade name, trademark, manufacturer, or otherwise, does not necessarily constitute or imply its endorsement, recommendation, or favoring by the United States Government or any agency thereof or its contractors or subcontractors. The views and opinions of authors expressed herein do not necessarily state or reflect those of the United States Government or any agency thereof.

Trademark Disclaimer

Reference herein to any specific commercial product, process, or service by trade name, trademark, manufacturer, or otherwise, does not necessarily constitute or imply its endorsement, recommendation, or favoring by the United States Government or any agency thereof or its contractors or subcontractors.

PPPL Report Availability

Princeton Plasma Physics Laboratory:

<http://www.pppl.gov/techreports.cfm>

Office of Scientific and Technical Information (OSTI):

<http://www.osti.gov/bridge>

Related Links:

[U.S. Department of Energy](#)

[Office of Scientific and Technical Information](#)

[Fusion Links](#)

Combined Ideal and Kinetic Effects on Reversed Shear Alfvén Eigenmodes*

N. N. Gorelenkov, G. J. Kramer, and R. Nazikian

*Princeton Plasma Physics Laboratory,
Princeton University, P.O.Box 451, 08543*[†]

Abstract

A theory of Reversed Shear Alfvén Eigenmodes (RSAEs) is developed for reversed magnetic field shear plasmas when the safety factor minimum, q_{min} , is at or above a rational value. The modes we study are known sometimes as either the bottom of the frequency sweep or the down sweeping RSAEs. We show that the ideal MHD theory is not compatible with the eigenmode solution in the reversed shear plasma with q_{min} above integer values. Corrected by special analytic FLR condition MHD dispersion of these modes nevertheless can be developed. Large radial scale part of the analytic RSAE solution can be obtained from ideal MHD and expressed in terms of the Legendre functions. The kinetic equation with FLR effects for the eigenmode is solved numerically and agrees with the analytic solutions. Properties of RSAEs and their potential implications for plasma diagnostics are discussed.

*This work supported by DoE contract No. DE-AC02-09CH11466.

[†]Electronic address: ngorelen@pppl.gov

I. INTRODUCTION

Theoretical and experimental studies of Alfvén plasma oscillations, known as Reversed Shear Alfvén Eigenmodes [RSAEs, dubbed as Alfvén Cascade (AC) modes] have attracted a lot of interest from the fusion community. Unstable RSAEs have been observed and identified on many tokamak devices [1–3]. Enhanced losses of fast ions were reported in plasmas with RSAEs present [4]. RSAE theory has been able to explain several puzzling features of TAE like instabilities in earlier TFTR observations [5]. Understanding RSAEs helps to study new physics of interactions between Alfvén and acoustic branches [6, 7]. Observations of RSAEs often serve as a useful diagnostic indicator of such things as (i) reversed safety factor profile in the plasma, $q(r)$, (ii) rational values of its minimum, q_{min} , and (iii) the formation of ITBs [8]. In many instances the accuracy of q_{min} from RSAE frequency measurements alone is expected to be greater than what follows from the direct measurements of the q profile with diagnostics like MSE (motion Stark effect). In general, both techniques are complementary.

Most often in the plasma discharge evolution RSAE frequencies increase from a minimum stationary value up to the TAE frequency [1]. In this paper we use the term “frequency sweep” for the phenomena of the identifiable RSAE frequency evolution which occurs on an equilibrium time scale. This should be considered distinct from the fast changing or “chirping” frequency magnetic activity which is understood to result from nonlinear wave particle dynamics. Theoretically and numerically, it was found that RSAEs exist in ideal MHD [9, 10] even when fast ion effects are ignored. The latter was argued originally to be the reason of RSAE existence [11, 12].

However, seemingly the same kind of RSAE instabilities, but with the frequency sweeping down (termed here down sweep) are also observed (see for example [10]). Such relatively rare events may be indicative of stronger damping, i.e. the instability is excited only when the drive is strong. Alternatively the rare existence of down sweep RSAEs may indicate that the criteria for such mode existence are more stringent than for the upsweeping modes. The second explanation seems to be consistent with our results reported here.

Two alternative theories were proposed recently to explain this phenomena. One is the unconventional theory of propagating “quasi”-modes resonantly excited by the fast trapped ions can explain the existence of the modes in the required frequency range [12, 13]. Another work is based on more conventional theory of Alfvénic eigenmodes in tokamaks [14].

This theory can explain both down sweep and sweep bottom modes (the latter are at the stagnating point of their frequency evolution). Still the existence condition and damping of such modes on the continuum are poorly described. In this paper we continue RSAE studies, which are consistent with the second argument.

Numerically, down sweep RSAEs were modeled with the code NOVA [15], where ideal MHD RSAEs structures were found for the down sweep and sweep bottom cases. In those simulations down sweep RSAE solutions were confirmed but required more deeper analysis in particular to understand the criteria of mode existence, which we offer in this paper. One explanation is that the NOVA results of Ref. [15] are not converged owing to the incorrect ideal MHD treatment of the singularities of the solutions at the interaction points with the Alfvén continuum.

Another work, Ref.[16], analytically finds strongly localized kinetic RSAEs (KRSAE) with the radial scale on the order of ρ_i , which are potentially stronger damped than the solutions found in our work. Found solutions are similar in localization as ones reported numerically [17] recently. The later reference shows solutions, which are similar to ours when the mode structure becomes narrow.

In this paper we have found analytically the existence conditions for down sweep and sweep bottom RSAEs. Our results, exact in certain cases, indicate that ideal MHD added by the kinetic theory can be used to find eigenmodes with the logarithmic asymptotic features. These results are consistent with the ideal MHD results of Ref. [15]. We call these solutions eigenmodes (hence, RSAEs) because their dispersion relations can be understood (and derived) in terms of the quantization condition between two points of a resonance with the continuum. We then compare the analytic results with direct numerical solutions of the eigenmode equation and with NOVA code solutions under such conditions when the proposed methods to solve the eigenmode equation are applicable, such as low beta, high aspect ratio plasma. The conditions for NOVA code applicability are discussed for more general plasma parameters. We explore the applicability of the ideal MHD theory to down sweep RSAEs. We have found a way to make a direct confirming comparison of RSAE long scale part of the solution with the kinetic one. Such analysis is also useful to understand whether down sweep RSAEs can be reproduced using the ideal MHD numerical codes. These ideal MHD results serve as limiting cases of the kinetic solutions.

In contrast to previous studies of KTAEs [18] and KRSAEs [16], down sweep and sweep

bottom RSAE solutions [14] considered here in details, maintain global structure even in the limit of vanishing FLR, which may have a profound effect on the fast ion and even the thermal plasma transport. It also follows that the global, large scale part of RSAE solution satisfies the ideal MHD dispersion equations. KTAEs and (K)RSAEs can be weakly damped, but are strongly localized in this limit.

The existence of singular eigenmodes in ideal MHD approximation are close to the results of Ref. [15]. We call these singular solutions eigenmodes (hence, RSAEs) because their dispersion relations can be understood in terms of the quantization condition between two points of a resonance with the continuum.

The paper is organized as follows. First we offer the derivation of RSAE eigenmode equation in section II. It is then analyzed in section III by employing different methods, including WKB, direct analytical solution, quadratic form minimization and numerical shooting technique. In the same section we obtain the expression for the damping rate of the RSAE solution. We compare solutions obtained with the NOVA code in section IV. We summarize and discuss results in the summary section V.

II. FORMULATION OF THE EIGENMODE EQUATION

We start with the eigenmode equation for the Alfvén oscillations [7, 19], which includes finite plasma pressure effects and is augmented by the FLR terms capable to mediate the ideal mode singularity,

$$\begin{aligned} & \hat{L}_4 \phi_0 + \hat{L} \phi_0 + \frac{\alpha m^2}{q_{min}^2} \left[2q_{min}^2 \frac{2\bar{\omega}^2 \Delta' - \alpha k_{00}^2}{1 - 4k_{00}^2 q_{min}^2} + \varepsilon \left(1 - \frac{1}{q_{min}^2} \right) \right] \phi_0 + \\ & + 2m^2 \left[\frac{\bar{\omega}^2 \varepsilon (\varepsilon + 2\Delta') - \delta_{m\partial} (-4\Delta' + \varepsilon + \alpha) (3\varepsilon - \alpha)}{1 - 4k_{00}^2 q_{min}^2} + \hat{Q}_k \right] \phi_0 = 0, \end{aligned} \quad (1)$$

where $\alpha \equiv -R_0 q_{min}^2 \beta'$, prime here and below denotes radial derivative, and $\delta_{m\partial} \equiv \partial_r^2 \phi_0 / (\partial_r^2 - m^2) \phi_0$, which is to be approximated as 1 if $\partial_r^2 \gg m^2$ and 0 if $\partial_r^2 \ll m^2$, i.e. two analytically treatable cases. Also here $\hat{L} = \partial_r [(\bar{\omega} + i\eta)^2 - k_0^2] \partial_r - m^2 [(\bar{\omega} + i\eta)^2 - k_0^2]$, $\partial_r = rd/dr$ operates on perturbed quantities. The frequency in Eq.(1) is generalized to include the upshift due to Geodesic Acoustic Mode (GAM) effect $\bar{\omega} \equiv R_0 \sqrt{\omega^2 - \omega_G^2} / v_A$ [20, 21], ω_G is the GAM frequency (applied to RSAE theory in Ref.[6]), v_A is local Alfvén velocity, $k_0 = m/q - n = m\iota - n$, $k_{00} = k_0(r_0)$, $\iota = 1/q$ is introduced for convenience, $\varepsilon = r/R_0$, Δ' is the radial derivative of the Shafranov shift, and the following anzats for the

perturbed quantities is assumed

$$\phi = e^{-i\omega t - in\zeta} \sum_j \phi_{j-m}(r) e^{ij\theta},$$

where the dominant harmonic is at $j = m$. Eq.(1) is derived in the vicinity of r_0 (see Refs. [7, 19] for details) where $q(r_0) = q_{min}$, so that the radial dependencies of different terms in this equation including $\omega_G(r)$ dependence are neglected, except for the $k_0(r)$, which is critical for the solution and is due to $q(r)$. This approach is valid for the localized modes, such as high- n modes. We will focus on the solutions at $\omega \geq \omega_G$. For the MHD eigenmodes below GAM frequency due to Alfvén acoustic coupling see Ref. [22]. Here we introduced intrinsic net drive term $\eta < 0$ (neglecting its radial variation), which may include both excitation and damping (following works [23, 24]). Exact form of η is not important for this paper, but its sign is important in evaluating the coupling of ideal to kinetic scales. The linear theory deals with the unstable modes near instability threshold, $0 < \gamma \equiv \Im\bar{\omega} \ll |\eta|$. This condition implies that the system has damping coming from either \hat{Q}_k term or from the radiative damping addressed here. Our theory will rely on the assumption that net intrinsic mode drive is smaller than the shift of the mode frequency from the continuum, $|\eta| \ll |\Re\bar{\omega} + k_{00}|$, as well as the frequency itself, $|\eta| \ll \Re\bar{\omega}$. The opposite case $|\eta| > |\Re\bar{\omega} + k_{00}|$ corresponds to strongly driven modes such as resonant modes.

FLR term \hat{L}_4 accounts for coupling to small scale KAW at the resonance with the continuum and is taken following Ref. [24, 25] $\hat{L}_4 = \partial_r \hat{\lambda}^{-2} \partial_r^3$, where

$$\hat{\lambda}^{-2} = [3(1 - i\delta_i)\bar{\omega}^2/4 + k_0^2(1 - i\delta_e)T_e/T_i] \rho_i^2/r_0^2 \ll 1, \quad (2)$$

and $\delta_{i,e} > 0$ are the dissipation terms from ions and electrons respectively. Another form of the FLR term is derived recently [26] can be used as well, but gives essentially the same results for high- n modes considered here. The derivation of Eq.(1) relied on one dominant m th and two sidebands, $m \pm 1$, harmonics, which accounted for up to ε^2 order corrections in the eigenmode equation.

The quantity \hat{Q}_k in Eq.(1) accounts for another kinetic effects, which may be responsible for the drive and damping of the RSAE instability. One of such effects could be due to fast ion gyro averaging as was suggested in Ref. [11].

In the vicinity of q_{min} we expand the resonant factor in front of the second derivative making use of $q'(r_0) = 0$. In addition we assume that the frequency is complex, denoting

$\bar{\omega}_r \equiv \Re \bar{\omega}$ and $\bar{\omega}_i \equiv \Im \bar{\omega}$, and demand that $|\bar{\omega}_i| \ll \bar{\omega}_r$. Then we can write

$$(\bar{\omega} + i\eta)^2 - k_0^2 = [\bar{\omega}_r^2 - k_{00}^2] [i\hat{\gamma} + 1 - Ax^2 - Bx^4], \quad (3)$$

where $x = (r - r_0) m/r_0$, $\hat{\gamma} = (\eta + \bar{\omega}_i) / (\bar{\omega}_r + k_{00})$,

$$\begin{aligned} A &= \frac{k_{00} t'' r_0^2}{m [\bar{\omega}_r^2 - k_{00}^2]}, \\ B &= \frac{t''^2 r_0^4 + k_{00} t'''' r_0^4 / 3m}{4m^2 [\bar{\omega}_r^2 - k_{00}^2]}, \end{aligned} \quad (4)$$

and derivatives are taken over r at $r = r_0$.

In evaluating the eigenmode dispersion we will use a convenient form of the safety factor profile [19], which is sufficiently general for high- n analysis of the localized eigenmodes

$$q(r) = \iota(r)^{-1} = \frac{q_{min}}{1 - (r - r_0)^2 / w^2}. \quad (5)$$

Here we express the q -profile width parameter w as $w^2 = 2q_{min} / q''|_{r=r_0}$. Coefficients A and B can be rewritten as:

$$\begin{aligned} A &= \frac{-k_{00} 2r_0^2}{mq_{min} w^2} \frac{1}{\bar{\omega}_r^2 - k_{00}^2} = -2k_{00} \sqrt{\frac{B}{\bar{\omega}_r^2 - k_{00}^2}} \\ B &= \frac{r_0^4}{m^2 q_{min}^2 w^4} \frac{1}{\bar{\omega}_r^2 - k_{00}^2} > 0 \end{aligned} \quad (6)$$

In a special case of down (up) sweep activity we have $q_{min} > m/n$ ($q_{min} < m/n$), $k_{00} < 0$ ($k_{00} > 0$), and $A > 0$ ($A < 0$), whereas at the sweep bottom $k_{00} = A = 0$. In all cases we assume $\bar{\omega}_r^2 > k_{00}^2$, as it was argued that $\bar{\omega}_r^2 < k_{00}^2$ is not suitable for the eigenmodes to exist [27].

Even though in experiments the down sweep instability continuously transforms to the sweep bottom and to the up sweeping one (see for example Ref.[19] for the structure in the latter case) their radial structures are different. The former two cases are the subject of this paper. It is convenient to write the resonant factor in the form

$$(\bar{\omega} + i\eta)^2 - k_0^2 = [\bar{\omega}_r^2 - k_{00}^2] D = [\bar{\omega}_r^2 - k_{00}^2] [(1 - z^2) (1 + \mu z^2) + i\hat{\gamma}], \quad (7)$$

where

$$z^2 = x^2 / S \equiv x^2 \left(\sqrt{1 + 4B/A^2} + 1 \right) A/2, \quad (8)$$

$\mu = \left(\sqrt{1 + 4B/A^2} - 1 \right) / \left(\sqrt{1 + 4B/A^2} + 1 \right)$, and for the special q -profile, Eq.(5), $\iota''' = \iota'''' = 0$ and $\mu = (\bar{\omega}_r + k_{00}) / (\bar{\omega}_r - k_{00})$. Eq.(7) includes information about the safety factor profile via k_{00} dependence only.

In contrast to the previous work [14] coefficients A, B, μ, S and radial variable z are defined real. This is more appropriate for the numerical analysis of the eigenmode equation presented here, but still can be used in the analytic analysis with the methods of Refs. [14, 28, 29].

The expression for S can be rewritten as follows:

$$S = \sqrt{\mu/B} = \frac{mq_{min}w^2}{r_0^2} (\bar{\omega}_r + k_{00}). \quad (9)$$

Using variable z we rewrite Eq.(1) in the form

$$L_4\phi_0 + L\phi_0 \equiv \left\{ \frac{\partial}{\partial z} \lambda^{-2} \frac{\partial^3}{\partial z^3} + \frac{\partial}{\partial z} D \frac{\partial}{\partial z} - SD + Q \right\} \phi_0 = 0, \quad (10)$$

where

$$\lambda^{-2} = \Lambda^{-2} \frac{\bar{\omega}^2}{(\bar{\omega}_r + k_{00})^2 (\bar{\omega}_r - k_{00})}, \quad (11)$$

$$\Lambda^{-2} = n(\rho_i^2/w^2) [3(1 - i\delta_i)/4 + (k_0^2/\bar{\omega}^2)(T_e/T_i)(1 - i\delta_e)],$$

$$Q = \frac{2S\hat{Q}}{\bar{\omega}_r^2 - k_{00}^2} = \frac{2mqw^2\hat{Q}}{r_0^2(\bar{\omega}_r - k_{00})}, \quad (12)$$

$$\hat{Q} = \alpha \left[\frac{2\bar{\omega}^2\Delta' - \alpha k_{00}^2}{1 - 4k_{00}^2q^2} + \frac{\varepsilon q^2 - 1}{2q^4} + \frac{\bar{\omega}^2 \varepsilon (\varepsilon + 2\Delta') - \delta_{m\partial} (-4\Delta' + \varepsilon + \alpha) (3\varepsilon - \alpha)}{\alpha (1 - 4k_{00}^2q^2)} \right] + \hat{Q}_k. \quad (13)$$

Here all radial dependencies are included via D term, and all other terms has to be evaluated at r_0 , so that here and below we use q instead of q_{min} . For the imaginary part of Q we can write

$$\Im Q \simeq \Im Q_k + \frac{4\bar{\omega}_i\bar{\omega}_r S}{\bar{\omega}_r^2 - k_{00}^2} \left[\frac{2\Delta'\alpha + \varepsilon(\varepsilon + 2\Delta') - \delta_{m\partial}(-4\Delta' + \varepsilon + \alpha)(3\varepsilon - \alpha)}{1 - 4k_{00}^2q^2} \right]. \quad (14)$$

In a special sweep bottom case, $\bar{\omega}_r^2 \gg k_{00}^2$, we find $S = 1/\sqrt{B} = \bar{\omega}_r mqw^2/r_0^2$, $\mu = 1$, and

$$Q_{bott} \simeq \frac{nw^2}{\bar{\omega}_r r_0^2} \alpha \varepsilon \frac{q^2 - 1}{q^2} + Q_k. \quad (15)$$

By making a special coordinate transformation we have found such a form of the ideal part of the eigenmode equation (last three terms in the brackets of Eq. (10)) which at sufficiently

small kinetic effects has parametric dependence only through two functions: S, Q . This is remarkable because the dispersion relation of RSAE solutions for any general case can be found as a parametric function of S and Q .

In the sweep bottom case the term responsible for the existence of RSAEs is coming from the averaged curvature (second term in square brackets of Eq.(13)) [7, 19]. It is clear that by choosing $\bar{\omega}$ small enough in sweep bottom case one can make Q value sufficiently large to create the effective potential well. It means that this case is compatible with the existence of the eigenmode and the instability is expected more reliably than in the case of the down sweep modes. Positive contribution from Q_k can also be considered favorable for the mode existence. At this point we finish the derivation of RSAE equation with thermal ion FLR term valid for the down sweep and sweep bottom cases.

III. SOLUTION TO THE RSAE EQUATION

In this section we solve the RSAE eigenmode equation, Eq.(10), and make their comparisons using several methods.

A. WKB RSAE analysis

It is important to perform a simple WKB analysis in order to develop an insight into the problem. We start with the formal WKB analysis of Eq.(10) by assuming $\bar{\omega}_i = 0$, $Q_k = 0$, and allowing the following ansatz dependence of the solution

$$\phi_0(z) = c_0 \exp\left(i \int^z k dz\right), \quad (16)$$

where c_0 is a proper dimensional constant, so that the eigenmode equation is transformed into

$$\frac{k^4}{\lambda^2} - Dk^2 - SD + Q = 0,$$

with the solution

$$k^2(z) = \frac{\lambda^2}{2} D \pm \lambda \sqrt{\lambda^2 D^2/4 + SD - Q}. \quad (17)$$

The WKB dispersion of RSAEs can be obtained from here by requiring $\int_{-1}^1 k(z=0) dz = \pi l$, where l is a positive integer, which should be large for WKB to be valid.

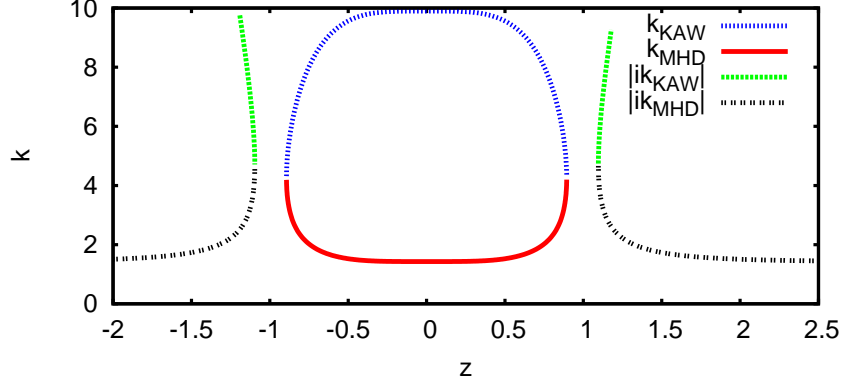


Figure 1: WKB wave vector solutions for the following set of parameters, $S = 2$, $Q = 4$, $\lambda = 10$, $\mu = 1$.

An example of two branches of these solutions is shown in Fig. 1. Both have an evanescent region outside and have wave-like regions inside $|z| = 1$.

Inside $|z| = 1$ the short wave component of the solution corresponds to the kinetic Alfvén wave (KAW) branch and is approximately

$$k_{KAW} = \lambda\sqrt{D}.$$

It is this branch, which is studied in Ref.[16]. It has the following dispersion relation

$$\lambda \simeq l\pi/2. \quad (18)$$

The second branch is characterized by the long wave scale and was considered in Ref.[14].

If $\lambda \gg 1$ this branch wavevector is given by

$$k(z) = \sqrt{\frac{Q}{(1-z^2)(1+\mu z^2)} - S}.$$

For the solution localized near $z = 0$, the condition $Q \gg S$ has to be satisfied, which is achievable for $\bar{\omega}$ sufficiently close to k_{00} :

$$\sqrt{Q - S} \simeq l\pi/2. \quad (19)$$

The condition $Q \gg S$, as we will see, is also a threshold condition for RSAE existence as it emerges from the continuum, i.e. when $\bar{\omega} \sim -k_{00}$ (see Eq.(9)).

Surprisingly, despite the WKB validity condition, $l \gg 1$, the dispersion relation, Eq.(19), is very close to the exact solution even for $l = 1$. As one may expect at $l = 1$ the down

sweep frequency is close to the continuum $(\bar{\omega}_r + k_{00})/\bar{\omega}_r \ll 1$. Both regions, near $|z| = 1$ and outside, $|z| > 1$, serve as evanescent regions for the solutions and do not effect the mode dispersion.

One particular case of practical importance, which is often verifiable in experiments is the sweep bottom solution. For this case using Eqs.(9,15,19) and retaining only real parts one can obtain the frequency upshift from the continuum

$$\bar{\omega}_{WKB} = -\frac{\pi^2}{2^3} \frac{r_0^2}{mqw^2} + \sqrt{\frac{\pi^4}{2^6} \frac{r_0^4}{m^2 q^2 w^4} + \frac{\alpha\varepsilon}{q^2} \left(1 - \frac{1}{q^2}\right)}. \quad (20)$$

At this point we immediately conclude one important consequence of this dispersion, that it predicts the disappearance of pressure gradient driven frequency upshift from the continuum if $q \simeq 1$. This important property agrees with observations reported recently on NSTX [30] (see Fig.3(a) of that paper, which indicates the convergence of RSAE frequencies at different n 's at $t = 0.35$, i.e. when $q_{min} = 1$).

Even though the RSAE solutions have singularities at $z = \pm 1$, their WKB dispersion is important for the insight. As we will show, the WKB dispersion gives an accurate value for the eigenfrequency in the case of the sweep bottom RSAEs.

The dispersion given by Eq.(20) is different from the one which follows from Eq.(1) if the radial derivative terms are neglected, which follows from the results of Refs.[7, 19]. Such approach can not provide the eigenmode structure, but can give an eigenfrequency limit value for the modes propagating primarily in the poloidal direction, that is when

$$k_\theta = m/r \gg k_{\theta crit} = \frac{\pi^2}{2^3} \frac{r_0}{w^2} \frac{q}{\sqrt{\alpha\varepsilon(q^2 - 1)}}. \quad (21)$$

In this case we find from Eq.(20):

$$\bar{\omega}^2 = \frac{\alpha\varepsilon}{q^2} \left(1 - \frac{1}{q^2}\right). \quad (22)$$

Such approach was employed in Ref.[12]. The difference with the more complete dispersion, Eq.(20), is due to the appropriate treatment of the radial scale length in the later, which is critical for the quantization condition of RSAEs.

We would like to point out another important and experimentally verifiable property of RSAE dispersion, which is the dependence of the mode frequency on the mode number. It is predicted by our dispersion, Eq.(20), and is absent in Eq.(22) and in Refs.[12, 13]. If the

fast ion shift is included, results of Refs.[12, 13] would give opposite m dependence, that is their results would give lower frequency for high m (and n) modes, which is at odds with our results and with the observations on NSTX [30] (Fig.3 of that reference).

We also find that in this case the characteristic mode width resulting from Eq.(8) with z ranging from -1 to 1 is

$$\Delta r = 2w \sqrt{\frac{\sqrt{\alpha\varepsilon(q^2 - 1)}}{mq}}. \quad (23)$$

In the opposite case of strongly localized solutions, $k_{\theta crit} \gg k_\theta$, we find

$$\bar{\omega} = \frac{4}{\pi^2} \frac{nw^2\alpha\varepsilon}{r_0^2} \left(1 - \frac{1}{q^2}\right), \quad (24)$$

and

$$\Delta r = \frac{4}{\pi} \frac{w^2}{r_0} \sqrt{\frac{\alpha\varepsilon(q^2 - 1)}{q^2}} = \frac{\pi}{2k_{\theta crit}}. \quad (25)$$

B. Ideal MHD limit of RSAE equation

It is well acknowledged Timofeev [31] that in general the ideal MHD is inadequate framework for an eigenmode solution due to the resonance with the Alfvén continuum. This was recently confirmed in a special case of down sweep and sweep bottom RSAEs [14]. Nevertheless a certain ideal solution with special boundary conditions exist and corresponds to the long radial scale part of the down sweep and sweep bottom RSAEs. Such solution results in RSAE existence condition and their dispersion relation. Introduction of the FLR effects helps to resolve the interaction with the continuum and are required to properly match both kinetic and ideal scales. Thus it is important to study MHD part of RSAEs in details. In addition it is especially important to understand the relevance of the considered RSAEs to the solutions obtained by the ideal MHD real frequency codes such as NOVA [32].

The ideal MHD limit of Eq.(10), i.e., $L\phi_0 = 0$, can be analyzed analytically for the down sweep case, $\mu \ll 1$, at near threshold existence condition, that is when the ideal mode emerges from the continuum and $\bar{\omega} \simeq -k_{00}$, $Q \gg S$. We rewrite the eigenmode equation near the point of expected mode localization, $z = 0$:

$$\frac{\partial}{\partial z} (1 - z^2 + i\hat{\gamma}) \frac{\partial}{\partial z} \phi_0 + (Q - S) \phi_0 = 0. \quad (26)$$

Real solutions of this equation satisfying zero boundary conditions at $z \rightarrow \pm\infty$ are Legendre

functions [33]

$$\phi_0 = c_0 Q_{l-1}(z), \quad (27)$$

where $l = \left[\sqrt{1 + 4(Q - S)} + 1 \right] / 2$, which implies that the dispersion in the down sweeping case is close to

$$Q - S = l(l - 1), \quad (28)$$

where l is a positive integer. Note, that the latter dispersion is close to WKB result of Eq.(19) in the limit of $Q \gg S, 1$, which implies high radial mode numbers should be $l \gg 1$.

Although the solution, Eq.(27), is symmetric and continuous everywhere except near $|z| = 1$, it is not physical for the reason that it can not satisfy the causality condition. Indeed let's construct an analytic continuation of the above solution into the complex plane. We apply the standard procedure with $\eta = 0$, $\bar{\omega}_r + k_{00} \gg \bar{\omega}_i > 0$, to integrate $L\phi_0 = 0$ through the singular points from $\pm(1 + \varepsilon)$ to $\pm(1 - \varepsilon)$ ($0 < \varepsilon \ll 1$). The rule can be obtained by employing the asymptotic of the Legendre function at the singularity

$$2Q_l(z) \simeq P_l(z) \ln(-1 \pm z) \rightarrow P_l(z) [\ln(1 \mp z) - i\pi]. \quad (29)$$

Owing to the opposite parities of Q_l and P_l , complex ideal solutions obtained this way approach the origin with discontinuities:

$$\phi_0 = c_0 \phi_{0M} \equiv c_0 \left[\Re Q_{l-1}(z) + \frac{i\pi H(1 - |z|) \text{sign}(z)}{2} \Re P_{l-1}(z) \right], \quad (30)$$

where H is the Heaviside step function. Only imaginary part of this function has discontinuity near the origin, which is in ϕ_0 for odd l or in ϕ'_0 for even l . Note that if l is not integer the discontinuity is in both ϕ_0 and ϕ'_0 . This can be seen from the figure 1 of Ref.[14]. Our argument is along the lines of the well known problem of the nonexistence of stable ideal MHD eigenmodes in a plasma with the nonuniform density [31]. FLR term is required in order to match ϕ'_0 at $z = 0$ (even l), but does not allow to match for odd l due to the jump in the real part of the solution.

Because of the importance of the MHD solution we refine its dispersion, Eq.(28), by employing the quadratic form minimization given the ansatz, Eq.(30). This procedure allows to write it in the form

$$Q - i_l S = 2l'(2l' - 1), \quad (31)$$

where for the lowest radial mode numbers $i_{\nu} = 0.401, 0.489, 0.496, \dots (l' = 1, 2, 3\dots)$, and

$$i_{\nu} = \int_{-\infty}^{+\infty} (1 - z^2) \phi_0^2 dz / \int_{-\infty}^{+\infty} \phi_0^2 dz \quad (32)$$

is evaluated numerically. In the sweep bottom case, $\mu = 1$, simple WKB dispersion, Eq.(19) (again similar to the down sweep case only even radial solutions should be used, $l = 2l'$), provides good approximation for the RSAE frequency. Direct application of the numerical shooting technique to equation $L\phi_0 = 0$ presented hereafter, shows good agreement with the dispersions Eq.(31,19) over the range of plasma parameters (see section IV).

C. Hybrid MHD/kinetic RSAE analytic solution

One class of solutions of Eq.(10) is found by matching the MHD part, Eq.(30), with the kinetic counterpart to regularize the abovementioned discontinuity in the derivative ϕ_0' near the origin. In this section we provide further details of the derivation of the solution in addition to those published before [14].

Coupling of the ideal part of the solution (long radial scale) and the KAW (short scale, see Fig.1) occurs in the nonideal region (see for example Refs.[28, 31]). The coupling strength computation of the present paper is relied upon the Orr-Sommerfeld equation analysis [28]. The dispersion relation of the final solution arises from the matching condition of the two solution asymptotics at large λ . The approximate solution structure also can be obtained.

Basing on the results of Refs.[28, 31] and on our WKB analysis we define three regions of z . First is the outer region (I) $|z| > 1 + \varepsilon$, where the solution is dominantly MHD one. Second region (II) is the nonideal region where the scales of the kinetic and MHD solutions approach each other $|z - 1| < \varepsilon$ (see Fig.1). The third region (III) is inner region $|z| < 1 - \varepsilon$, which is wave - like for both MHD and KAW solutions, where the characteristic value of the nonideal region width is $\varepsilon = O(\lambda^{-2/3})$.

In region II with the help of the substitution $y = 1 + i\hat{\gamma}/p \mp z$ we rewrite the eigenmode equation near continuum resonance points $y = 0$ ($z = \pm 1$)

$$\left\{ \frac{\partial^4}{\partial y^4} + p\lambda^2 \left[y \frac{\partial}{\partial y^2} + \frac{\partial}{\partial y} + \frac{Q}{p} \right] \right\} \phi_0 = 0, \quad (33)$$

where $p = 2$ for down sweep mode or $p = 4$ for sweep bottom cases. From Eqs.(8,9) and $0 < \bar{\omega}_i \ll -\eta \ll \bar{\omega} + k_{00}$ it follows that $\Im y < 0$ in the vicinity of $z = \pm 1$. Also from Eq.(11)

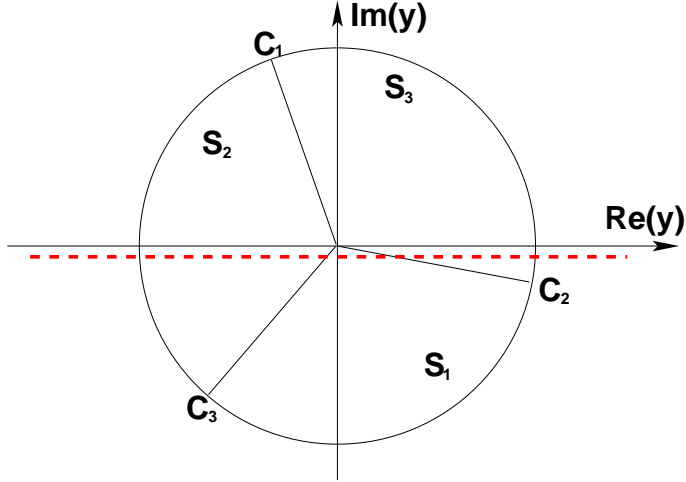


Figure 2: Diagram of various regions in complex y plane for the choices of various linear independent solutions as per Ref.[28]. Dashed line corresponds to the integration path.

it follows that $\Re\lambda \gg \Im\lambda > 0$ for both down sweep and sweep bottom cases. This is different from Ref.[14] due to allowed damping from the finite collisional terms $\delta_{i,e} \gg \bar{\omega}_i > 0$ and different coordinate transformation, Eq.(3).

Based on the signs of λ and y we show the diagram for the choice of the linear independent solutions according to Ref.[28] in Fig. 2. Argument of the ray C_2 equals to $-2 \arg \lambda/3$, which and the rays $C_{1,3}$ are shifted by 120 degrees from each other. Sector S_2 outside the circle corresponds to the region I, outer sector S_3 corresponds to region III, and the inner circle S to region II in our definition.

At $\lambda \gg 1$ we choose following two solutions, which we require to be limited along the line of the integration on both sides outside of the circle S :

$$b_0/2\pi i = J_0 \left(2\sqrt{Qy/p} \right) \quad (34)$$

and B_3 , which in a sector S_2 takes the form

$$B_3 = \pi i H_0^1 \left(2\sqrt{Qy/p} \right), \quad (35)$$

and in a sector S_3

$$B_3 = \frac{-\sqrt{\pi} e^{-3i\pi/4}}{p^{1/4} \lambda^{1/2} y^{3/4}} e^{-2\lambda\sqrt{p}y^{3/2}i/3} + \pi i H_0^1 \left(2\sqrt{Qy/p} \right). \quad (36)$$

We can thus find the following connecting formulas for the solutions near $y = 0$ for $b_0/2\pi i$

and B_3 :

$$\pi i - \left[\ln \left(-\frac{yQ}{p} \right) + 2\gamma \right] \overset{1 \leftrightarrow 1}{\leftrightarrow} - \left[\ln \left(\frac{yQ}{p} \right) + 2\gamma + \frac{\sqrt{\pi} e^{-3i\pi/4} e^{-2\lambda\sqrt{p}y^{3/2}i/3}}{p^{1/4}\lambda^{1/2}y^{3/4}} \right], \quad (37)$$

where γ is the Euler's constant. The linear combination of two independent solutions,

$$-B_3 + \frac{b_0}{2\pi} \left[\pi + i2\gamma + i \ln \left(\frac{Q}{p} \right) \right],$$

has MHD scale at $\Re y < 0$ and mixed MHD/KAW scale at $\Re y > 0$ (cf. Ref.[14])

$$\ln(-y) \leftrightarrow \ln(y) + \pi i + \frac{\sqrt{\pi} e^{-3i\pi/4} e^{-2\lambda\sqrt{p}y^{3/2}i/3}}{p^{1/4}\lambda^{1/2}y^{3/4}}. \quad (38)$$

In region III the standard WKB analysis produces solutions for the short scale wavevector $k(z) = \pm\lambda\sqrt{D} + 3i\partial_z [\ln(\lambda^2 D)]/4$ and the corresponding solutions are

$$\phi_{0f} = \frac{C}{\lambda^{3/2}D^{3/4}} e^{-3i\pi/4 \pm i \int \lambda\sqrt{D} dz}. \quad (39)$$

The choice of the signs in the exponent and the constant C are determined by matching conditions with the asymptotics Eq.(38) at $z = \pm 1$:

$$\phi_{0f} = \frac{\sqrt{p\pi}\lambda_{\pm 1}}{2\lambda^{3/2}D^{3/4}} e^{-3i\pi/4 \mp i \int_z^{\pm 1} \lambda\sqrt{D} dz}. \quad (40)$$

where subscript ± 1 (signs \pm will be dropped hereafter) means that the value is taken at the nonideal region, i.e. at the point of the mode frequency resonance with the continuum.

Final solutions is

$$\phi_0 = c_0 [\phi_{0M}^* - \phi_{0f}]. \quad (41)$$

From matching the first derivatives of the left and right solutions near origing $z = 0$ the following condition emerge

$$[-i\pi c_M/2 + \phi'_{0f}(0 - \varepsilon)]|_{\varepsilon \rightarrow 0} = [i\pi c_M/2 + \phi'_{0f}(0 + \varepsilon)]|_{\varepsilon \rightarrow 0}, \quad (42)$$

where

$$c_M = P'_{2l'-1} = (-1)^{l'+1} (l' - 1/2)! / (l' - 1)! (1/2)!. \quad (43)$$

The real part of it is

$$\Re \int_0^1 \lambda\sqrt{D} dz = 2\pi \left(j + \frac{1}{8} \right). \quad (44)$$

where $j \gg 1$ is an integer, and its imaginary part describes the effect of the dissipation

$$\Im \int_0^1 \lambda \sqrt{D} dz = \ln \frac{c_M \sqrt{\lambda_0 \pi}}{\lambda_1 \sqrt{p}}. \quad (45)$$

As we have shown Eq.(38) is valid for both down sweep and sweep bottom cases. The matching condition is essentially the same for the sweep bottom case as we verified numerically for low l' values.

The real part of the kinetic dispersion relation alludes to the splitting of the eigenmode frequency due to small scales. To find it we make use of the approximation in the integrand of Eqs.(44,45):

$$\sqrt{D} \simeq \sqrt{1 - z^p} + \frac{i\hat{\gamma}}{2\sqrt{1 - z^p}}. \quad (46)$$

From Eq.(44) we find the fine kinetic frequency splitting

$$\Delta \bar{\omega}_K = 4p \sqrt{p \bar{\omega}_r} \Re \Lambda_0^{-1} \left[4 - p + (p - 2) \frac{2}{3\sqrt{\pi}} \frac{\Gamma(\frac{1}{4})}{\Gamma(\frac{3}{4})} \right]^{-1},$$

where $\Re \Lambda_0^{-1} = \frac{\rho_i \sqrt{n}}{w} \sqrt{\frac{3}{2} + \frac{T_e}{T_i} \frac{4-p}{2}}$, and Γ is the gamma function. From this splitting the number of linear submodes near the MHD frequency was found[14]:

$$N_{kRSAE} = \frac{(\bar{\omega} + k_{00}) \Re \Lambda_0}{\left(0.4S + Q \frac{\bar{\omega} + k_{00}}{\bar{\omega} - k_{00}}\right) \left| \ln \left(\frac{\eta}{\bar{\omega} + k_{00}} \right) \right| 4p \sqrt{p \bar{\omega}}} \left[4 - p + \frac{2}{3\sqrt{\pi}} \frac{\Gamma(\frac{1}{4})}{\Gamma(\frac{3}{4})} (p - 2) \right]. \quad (47)$$

We note that this expression is valid if $N_{kRSAE} \gg 1$ and otherwise the numerical solution should be considered.

One important feature of this solution is that instead of using standard causality condition with $\bar{\omega}_r \gg \bar{\omega}_i > 0$ we need to allow for the weakly unstable modes, that is with finite $0 < \bar{\omega}_i \ll -\eta \ll \bar{\omega}_r + k_{00}$. This is very important difference from the perturbation theory assumption and relies on the underlying threshold condition for the instability when the drive is sufficiently strong to overcome the intrinsic ‘‘radiative’’ damping.

From the equation (45) it follows the expressions for various components of the mode growth rate, which can be cast into a form:

$$\bar{\omega}_i = -\eta + \gamma_{rad} + \gamma_{diss},$$

where the radiative collisionless damping rate is

$$\gamma_{rad} = \frac{4\sqrt{2}}{\pi \Re \Lambda_0} \frac{\sqrt{\bar{\omega}_r} \ln(c_M \sqrt{\lambda_0 \pi} / \lambda_1 \sqrt{p})}{4 - p + \frac{\Gamma(\frac{1}{4})}{2\sqrt{2\pi}\Gamma(\frac{3}{4})} (p - 2)}, \quad (48)$$

and the dissipative damping on electrons and ions, such as due to collisions or Landau damping mechanism is

$$\frac{\gamma_{diss}}{\bar{\omega}_r + k_{00}} = -\frac{\delta_i \frac{3}{4} + \frac{T_e}{T_i} \frac{4-p}{2} \delta_e}{\frac{3}{4} + \frac{T_e}{T_i} \frac{4-p}{2}} \left[\frac{4-p}{2} + (p-2) \frac{2}{3} \right]. \quad (49)$$

We should note that the damping rate, Eq.(48), contains more accurate numerical factor than was obtained previously in Ref.[14], where the following approximation $\sqrt{D} = \sqrt{p(1 - i\hat{\gamma} + z)}$ was used instead of Eq.(46). Both give the same real part, whereas the imaginary part from Eq.(46) obtained here is more accurate.

The radiative damping rate to the lowest order depends on the ideal parameters Q and S via the mode eigenfrequency.

D. Numerical verification of RSAEs dispersion

Here we employ another, more direct method of solving for bottom RSAEs via numerical shooting of Eq.(10). For the sake of simplicity in the verification exercise we assume that

$$\Lambda^{-2} = \lambda^{-2} (1 - i\delta),$$

where we ignore the radial dependence of Λ . It is important that the eigenmodes remain near threshold, which is enforced in the numerical search for the solution by adjusting the free parameters of the equations. And, thus, δ should not be too small, but should have η drive term, which is adjusted in order to maintain $0 < \bar{\omega}_i \ll -\eta$.

In the parameter range of the plasma under consideration radiative damping is typically small. In the simulations we can find it by varying λ and seeking the asymptotic behaviour of both terms predicted by theory. From Eqs.(48,49) it is possible to separate the radiative damping from the total damping of the eigenmode solution. We demonstrate this for the sweep down case, for which one can find $\gamma_{rad} \sim \lambda^{-1} \ln \lambda$, whereas γ_{diss} does not depend on λ if $\bar{\omega}_r + k_{00}$ is kept constant. More explicitly we find the following dependencies of the damping rates on λ from Eqs.(43,48,49)

$$\frac{\gamma_{rad}}{\bar{\omega}_r} + \frac{\gamma_{diss}}{\bar{\omega}_r} = \frac{\sqrt{2}}{\pi \lambda \sqrt{\bar{\omega}_r}} \ln \left(\frac{\pi}{\lambda 2} \right) - \frac{\bar{\omega}_r + k_{00}}{\bar{\omega}_r} \delta, \quad (50)$$

In the case we analyze the RSAE modes have finite number of nodes, i.e. finite radial mode number. As the radial mode number increases, Q becomes sufficiently large and the

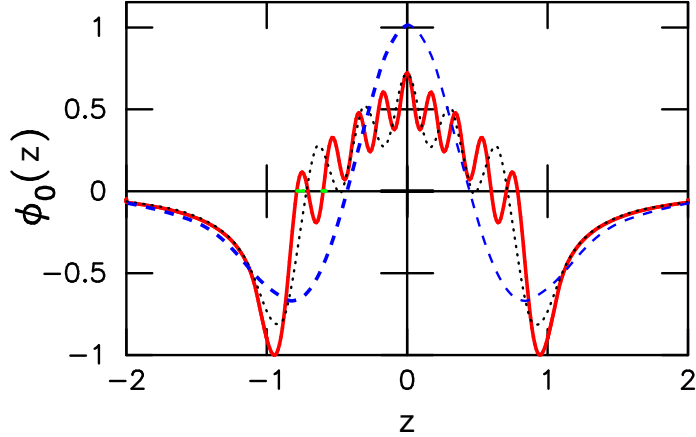


Figure 3: Lowest mode number sweep down RSAE structures obtained using the shooting technique. Shown are the first (dashed), third (points) and fifth (solid line) RSAEs.

mode existence condition is violated according to Eq.(31). This is confirmed numerically and limits the applicability of the dispersion equation (31). Numerically it is difficult to maintain the dispersion relation Eq.(31) especially in the sweep down case, so that there is always a finite number of radial nodes present even for the relatively high m number of 21. We rely in this case on the above WKB dispersion.

We choose basic plasma parameters corresponding to tokamak ordering [19] $R_0 = 10m$, $R/a = 10$, $q_{min} = 2.02$ at $r/a = 0.5$, $w = 0.9$, $\beta_0 = 0.1\%$, parabolic pressure profile, constant density profile, and $n = 10$. With these parameters we find $k_{00} = -0.024939$ and the eigenmode existence conditions.

At such parameters we find down sweep RSAEs satisfying existence condition which follows from the MHD scale structure, Eq.(31). Numerically we have found that only the most localized solutions satisfy it with the mode frequencies close to the MHD theoretical value.

For chosen parameters we have found the following examples of the down sweep RSAEs shown on Fig. 3. Their frequencies start from a value equal approximately to the continuum and increase as the mode becomes more global. The modes are plotted vs. the radial - like variable z . According to Eq.(8) it is connected to the radial space variable in such a way that the first lowest radial mode number RSAE is the most localized.

We also check the kinetic damping rate dependence on the radial mode number. For the kinetic damping rate we use expression derived above, which includes such effects as

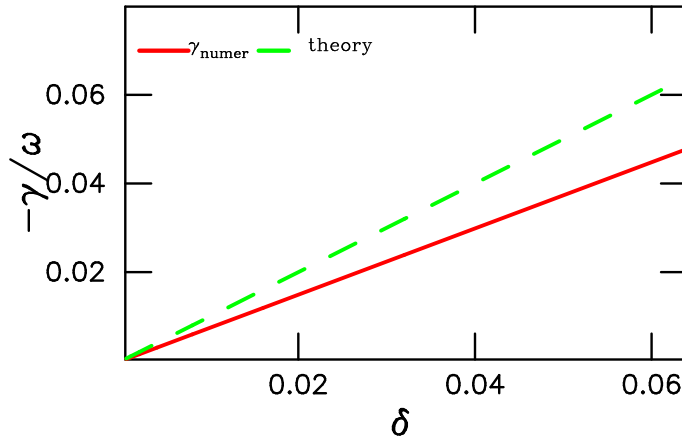


Figure 4: Down sweep RSAE damping rate as a function of the collisionality parameter δ (in our case).

collisional dissipation, Eq.(50). It is shown on the next figure 4.

Even though the kinetic expressions are more difficult to analyze they are expected to give more exact results than MHD theoretical values. Nevertheless making use of the MHD results is often helpful. Without the detailed kinetic analysis of the stability problem one can draw preliminary conclusions about the stability properties based on the MHD solutions. This may not be always accurate, but often is sufficient.

IV. RSAES IN IDEAL MHD CALCULATIONS

As we have mentioned ideal MHD RSAE analysis is important and often is a key to assess and understand the stability problems. Here we study properties of RSAEs from the MHD point of view. MHD limit provides the real part of the solution (large scale part) and the corresponding dispersion 31.

In order to formulate the MHD problem we impose special boundary conditions, which have zero function derivative in the origin and goes to zero in the infinity. We should note that this condition is not physical by itself due to the jumps of the function in the origin. However as we saw its dispersion can provide a good guess for the mode frequency. We argue

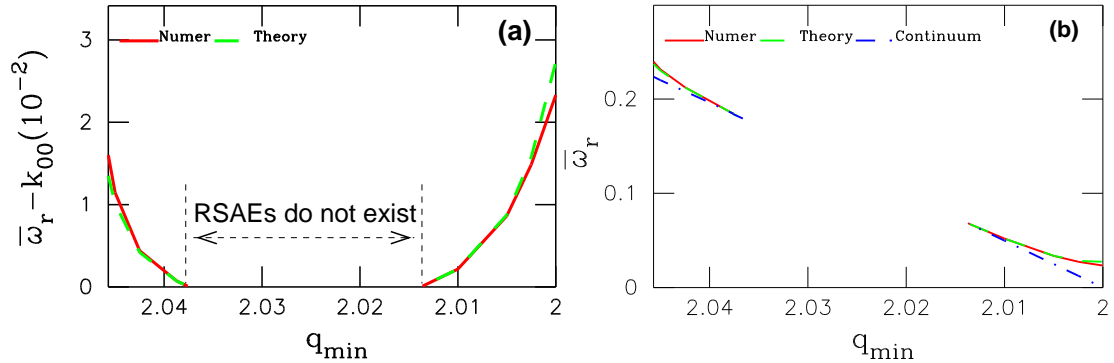


Figure 5: RSAE eigenfrequency obtained from the analytical dispersion (dashed line), Eq.(31), and from numerical shooting technique simulations (solid lines). The differences between the eigenfrequencies and the continuum frequencies are shown on the left figure and the absolute value of RSAE eigenfrequencies are shown on the right figure. For the comparison the TAE frequency in the normalized units is $\bar{\omega}_{rTAE} = 1/2q_{min} \simeq 1/4$.

that this dispersion can help to find a relatively quick way for RSAE stability analysis.

We again choose the same basic plasma parameters corresponding to the tokamak ordering $R_0 = 10m$, $R/a = 10$, $r/a = 0.5$, $w = 2$, $\beta_0 = 0.1\%$, parabolic pressure profile, constant density profile, and $n = 10$. Direct application of the shooting technique to RSAE equation (26) is important to understand the solubility condition for RSAE eigenproblem. Its solution is illustrated on Fig.5.

The figure 5 demonstrates the ideal MHD RSAE dispersion. One surprising following conclusion is that the ideal RSAEs do not always exist. In plasma parameters which we employ there is a range of plasma safety factor profile values q_{min} which does not allow the MHD part to exist. Nevertheless the mode frequency is still close to the continuum as can be seen from fig.5(b).

We are showing for the first time that RSAEs do not exist at certain q_{min} values due to the choice of plasma parameters. The reason is very simple. The slow growing part of the mode structure can not be formed at such parameters.

Finally, we simulate the RSAEs using the ideal MHD code NOVA [34]. NOVA employs a set of cubic polynomial finite elements to represent its solution and to solve a more complete system of ideal MHD equations. Since exact solutions have strong logarithmic singularities one should not expect that an ideal code such as NOVA will have converged solution for the

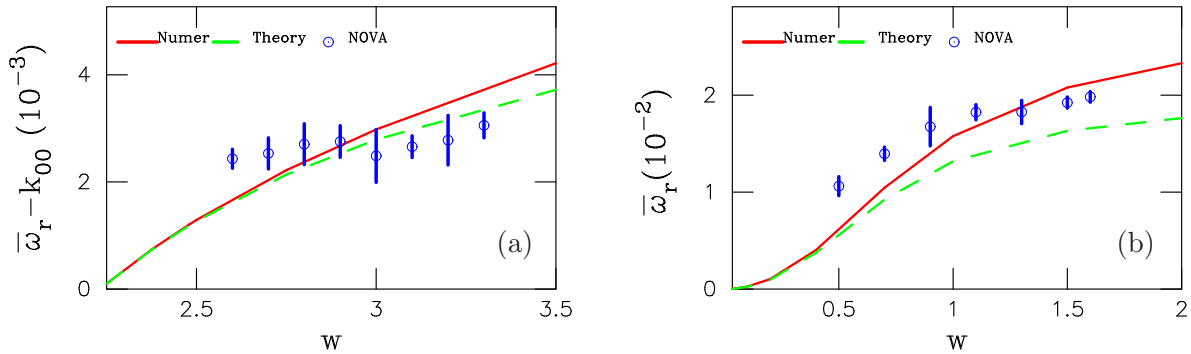


Figure 6: Down sweep RSAE eigenfrequency (Eq.(31, $q_{min} = 2.02$), figure (a)) and sweep bottom mode eigenfrequency ($q_{min} = 2$, figure (b)) are compared with numerical simulations of the growth rates. Only the difference between the eigenfrequency and the continuum frequency at q_{min} is shown. RSAE eigenfrequencies as computed with NOVA are shown as circles. A number of similar solutions were found with NOVA near the frequency range indicated with the vertical bars around the circles. The safety factor is $q_{min} = 2.02$.

down sweep and sweep bottom RSAEs. However, the regions where the solution is not well approximated is very narrow in radial direction. Therefore, one can ask: how good does NOVA approximate the solution we found analytically. We address this problem hereafter.

We compare the RSAE mode eigenfrequencies computed using NOVA code with the predicted mode frequencies computed numerically using the shooting algorithm in Figs. 6. NOVA finds RSAE modes within a certain range of w values. At lower limit of this range the eigenmode becomes too narrow to resolve. At higher limit of w range a problem of resolving the RSAE structure near the singular layer appears.

It can be seen from these figures that NOVA can find good approximations for the RSAE eigenfrequencies because as we saw the mode dispersion is determined by the “effective” potential well between two points of the resonance with the continuum. Numerically in NOVA simulations we found that for each w value there is a narrow range of frequencies where NOVA has several solutions (2 – 5 solutions at chosen parameters) with almost the same radial structure. These frequency ranges are shown in Figs. 6 as vertical lines with the median point shown as a circle. In these simulations, within the localization region of each mode we had approximately 150 radial grid points. A comparison of corresponding radial structures in the case of the sweep bottom RSAE is shown in Fig. 7, where RSAE

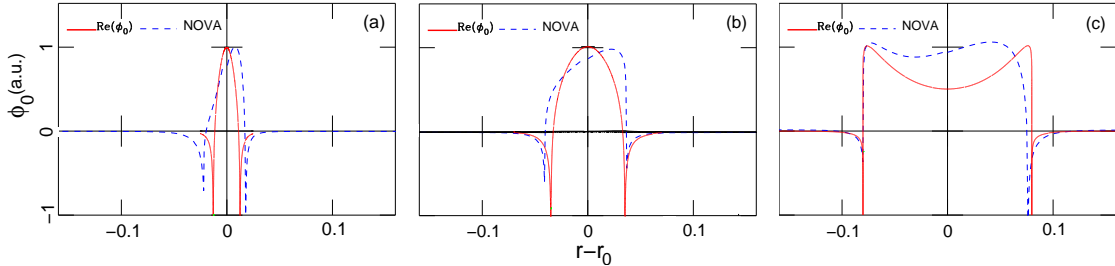


Figure 7: Sweep bottom RSAE mode dominant harmonic radial structures computed using the shooting numerical scheme and using NOVA ideal MHD code, as indicated. Figs. (a,b,c) correspond to three values $w = 0.5, 0.9, 1, 7$, respectively, and $q_{min} = 2$. The shooting scheme RSAE structures have both real and imaginary parts as indicated.

structures with the frequency at the median point were taken. It can be seen that NOVA solutions have the same singular-like structures as the shooting solutions. The difference of the location of the singularities is due to the difference in the mode frequencies. This difference in part is due to the finite radial resolution on both ends of shown w range. The differences in models and equilibria may also play a role. We also note that because of our normalization of the radial scale the solutions radial localization looks alike in z , whereas it is different in r .

A. Sweep bottom RSAE existence criterion

One important condition follows from our study is the existence criterion of the down sweep RSAEs which determines the plasma parameter space when the eigenfrequency is above the continuum, that is $\bar{\omega} > k_{00}$ and according to which the effective potential well of the eigenmode equation can be formed. The threshold condition can be approximated as $\bar{\omega} \simeq -k_{00}$, which implies $S \simeq 0$ for the down sweep RSAEs. One consequence of this is that the MHD dispersion near the threshold of down sweep RSAEs is exact. On the other hand, one can see from Eqs.(9,15) that for the sweep bottom RSAE, $k_{00} = 0$, there is no such threshold. That is formally at any w one can find a sufficiently small value of $\bar{\omega}_r$ that Q is sufficiently large and S is sufficiently small that the sweep bottom RSAE always exists. Hence, one can conclude that the sweep bottom RSAE instability is determined by the balance of the drive and damping.

Quantitatively the threshold condition for the down sweep RSAE follows from Eq.(31), which can be rewritten in the form $\Re(Q_{cr} + \langle Q_k \rangle) > 2$. This threshold can be sensitive to kinetic modifications of the eigenmode equation coming from fast ions (last term in the RHS). So testing the threshold by modifying the fast ion response in experiments can shed light on the physics of fast ion effects on RSAE formation. If k_{00} value at the threshold is close to the bottom, but finite, we can find the threshold frequency:

$$\bar{\omega}_{rth} = -k_{00} = \frac{nw^2}{r_0^2} \frac{\epsilon\alpha}{2} \frac{q^2 - 1}{q^2} (2 - \Re\langle Q_k \rangle)^{-1}.$$

It can be seen that this value is directly connected to the characteristic flatness of the safety factor profile, w . The observations of $\bar{\omega}_{rth}$ can also serve as a useful diagnostic tool. Note, that in this paper the characteristic width of the q profile is expressed via the second derivative of $q(r)$: $w^2 = 2q/q''|_{r=r_0}$ or $w^2 = -2/q\epsilon''|_{r=r_0}$.

V. SUMMARY

In this paper we presented a theory of down sweep and sweep bottom RSAE solutions using the kinetic and MHD frameworks. The theory allows to find RSAE radial structures, frequency dispersions, and the dissipative damping rates due to the interaction with the continuum in low beta and high aspect ratio plasma. It turns out that the radiative damping rate can be small for the modes in the limit of small FLR. A comparison with the numerical solutions of the reduced eigenmode equation using the shooting technique helps to validate the theoretical results.

We argue that the developed theory is supported by the experimental data of the observed modes in reversed plasmas. Indeed NSTX observations show that the frequency of RSAEs correlates strongly with the q -profile evolution as discussed in Sec.III A. It follows from the measurements that as q_{min} approaches 1 the frequency of the instability identified as RSAE, approaches the computed frequency of the continuum. At $q_{min} \sim 1$ the frequency of different n RSAEs becomes very close to each other after the correction due to the rotation is included. Our theory seems to be a rare one, which can explain this at the moment.

Developed theory helps to understand the range of ideal MHD codes applicability. Finding the RSAE solution in the cases considered in this paper appears to be a challenging problem for ideal MHD finite element codes such as NOVA. Because of the present singu-

larities NOVA can give good approximation to the long scale RSAE solution in the cases of bottom sweep and sweep down. Both the mode structure and eigenfrequency seems to be in an approximate agreement with the analytical solution we found.

With this understanding and depending on the application, NOVA can be applied to the analysis of down sweep and sweep bottom RSAEs observed in experiments. Obtained accurate dispersion relation for the sweep bottom RSAEs, Eq.(20), seems to be important for the comparisons with the experiment in which the finite pressure and pressure gradient effects should be separated. RSAE dispersion is also important for the applications to MHD spectroscopy, which seems to be possible by measuring the minimal point of RSAE frequency sweep. However experimental validation of the theory we presented is required.

Enlightening and motivating discussions with Dr. L.E. Zakharov are appreciated.

-
- [1] S. E. Sharapov, B. Alper, H. L. Berk, D. N. Borba, B. N. Breizman, C. D. Challis, A. Fasoli, N. C. Hawkes, T. C. Hender, J. Mailloux, S. D. Pinches, and D. Testa, *Phys. Plasmas* **9**, 2027 (2002).
 - [2] R. Nazikian, B. Alper, H. L. Berk, D. Borba, C. Boswell, R. Budny, K. Burrell, C. Cheng, E. Doyle, E. Edlund, R. J. Fonck, A. Fukuyama, N. N. Gorelenkov, C. M. Greenfield, D. J. Gupta, M. Ishikawa, R. J. Jayakumar, C. J. Kramer, Y. Kusama, R. J. La Haye, G. R. McKee, W. A. Peebles, S. D. Pinches, M. Porkolab, J. Rapp, T. L. Rhodes, S. E. Sharapov, K. Shinohara, J. A. Snipes, W. M. Solomon, E. J. Strait, M. Takechi, M. A. Van Zeeland, W. P. West, K. L. Wong, S. Wukitch and, L. Zeng, *Proceedings of 20th IAEA Fusion Energy Conference, Vilamoura, Portugal* (2004), IAEA-CN-116/EX/5-1, pp. 1–9.
 - [3] E. D. Fredrickson, N. A. Crocker, N. N. Gorelenkov, W. W. Heidbrink, S. Kubota, F. M. Levinton, H. Yuh, J. E. Menard, and R. E. Bell, *Phys. Plasmas* **14**, 102510 (2007).
 - [4] W. W. Heidbrink, N. N. Gorelenkov, Y. Luo, M. A. Van Zeeland, R. B. White, M. E. Austin, K. H. Burrell, G. J. Kramer, M. A. Makowski, G. R. McKee, and R. Nazikian, *Phys. Rev. Lett.* **99**, 245002 (2007).
 - [5] R. Nazikian, G. J. Kramer, C. Z. Cheng, N. N. Gorelenkov, H. L. Berk, and S. E. Sharapov,

- Phys. Rev. Lett. **91**, 125003 (2003).
- [6] B. N. Breizman, S. E. Sharapov, and M. S. Pekker, Phys. Plasmas **12**, 112506 (2005).
- [7] G. Y. Fu and H. L. Berk, Phys. Plasmas **13**, 052502 (2006).
- [8] E. Joffrin, A. C. C. Sips, J. F. Artaud, A. Becoulet, L. Bertalot, R. Budny, P. Buratti, P. Belo, C. D. Challis, F. Crisanti, M. de Baar, P. de Vries, C. Gormezano, C. Giroud, O. Gruber, G. T. A. Huysmans, F. Imbeaux, A. Isayama, X. Litaudon, P. J. Lomas, D. C. McDonald, Y. S. Na, S. D. Pinches, A. Staebler, T. Tala, A. Tuccillo and , K.-D. Zastrow, Nucl. Fusion **45**, 626 (2005).
- [9] B. N. Breizman, H. L. Berk, M. S. Pekker, S. D. Pinches, and S. E. Sharapov, Phys. Plasmas **10**, 3649 (2003).
- [10] G. J. Kramer, R. Nazikian, B. Alper, M. de Baar, G.-Y. Fu, N. N. Gorelenkov, G. McKee, S. D. Pinches, T. L. Rhodes, S. E. Sharapov, W. M. Solomon, and M. A. Van Zeeland, Phys. Plasmas **13**, 056104 (2006).
- [11] H. L. Berk, D. N. Borba, B. N. Breizman, S. D. Pinches, and S. E. Sharapov, Phys. Rev. Letters **87**, 185002 (2001).
- [12] B. N. Breizman, AIP conf. proceedings **871**, 15 (2006).
- [13] I. Abel, B. Breizman, and S. Sharapov, Phys. Plasmas **16**, 1?? (2009).
- [14] N. N. Gorelenkov, Phys. Plasmas **15**, 110701 (2008).
- [15] G. J. Kramer, N. N. Gorelenkov, R. Nazikian, and C. Z. Cheng, Plasma Phys. Contr. Fusion **46**, L23 (2004).
- [16] S. V. Konovalov, A. B. Mikhailovskii, M. S. Shirokov, E. A. Kovalishen, and T. Ozeki, Phys. Plasmas **11**, 4531 (2004).
- [17] G. Y. F. L. Yu and Z. M. Sheng, Phys. Plasmas **16**, 072505 (2009).
- [18] R. R. Mett and S. M. Mahajan, Phys. Fluids B **4**, 2885 (1992).
- [19] N. Gorelenkov, G. Kramer, and R. Nazikian, Plasma Phys. Control. Fusion **48**, 1255 (2006).
- [20] C. Z. Cheng, Phys. Fluids B **2**, 1427 (1990).
- [21] M. S. Chu, J. M. Greene, L. L. Lao, A. D. Turnbull, and M. S. Chance, Phys. Fluids B **4**, 3713 (1992).
- [22] N. N. Gorelenkov, H. L. Berk, E. Fredrickson, and S. E. Sharapov, Phys. Lett. A **370/1**, 70 (2007).
- [23] A. B. Mikhailovskii, [Sov. Phys. JETP **41**, 890 (1975)] Zh. Eksp. Teor. Fiz. **68**, 1772 (1975).

- [24] M. N. Rosenbluth and P. H. Rutherford, *Phys. Rev. Lett.* **34**, 1428 (1975).
- [25] A. Hasegawa and L. Chen, *Phys. Rev. Letter* **35**, 370 (1975).
- [26] G. Y. Fu, H. L. Berk, and A. Pletzer, *Phys. Plasmas* **12**, 082505 (2005).
- [27] S. E. Sharapov, A. B. Mikhailovskii, and G. T. A. Huysmans, *Phys. Plasmas* **11**, 2286 (2004).
- [28] A. L. Rabenstein, *Arch. Ratl. Mech. Anal.* **1**, 418 (1958).
- [29] A. L. Peratt and H. H. Kuehl, *Phys. Fluids* **15**, 1117 (1972).
- [30] N. Crocker, E. Fredrickson, N. Gorelenkov, G. Kramer, D. D. H. Heidbrink, S. Kubota, F. Levinton, H. Yuh, J. Menard, B. LeBlanc, and R. E. Bell, *Phys. Plasmas* **15**, 102502 (2008).
- [31] A. V. Timofeev, in *Reviews of Plasma Physics*, edited by M. A. Leontovich (Consultants Bureau, New York, 1986), vol. 9, pp. 265–298.
- [32] C. Z. Cheng and M. S. Chance, *Phys. Fluids* **29**, 3695 (1986).
- [33] M. Abramowitz and I. A. Stegun, *Handbook of mathematical functions* (National Bureau of Standards, Washington, USA, 1972), tenth ed., ISBN 0-486-61272-4.
- [34] C. Z. Cheng, *Phys. Reports* **211**, 1 (1992).

The Princeton Plasma Physics Laboratory is operated
by Princeton University under contract
with the U.S. Department of Energy.

Information Services
Princeton Plasma Physics Laboratory
P.O. Box 451
Princeton, NJ 08543

Phone: 609-243-2245
Fax: 609-243-2751
e-mail: pppl_info@pppl.gov
Internet Address: <http://www.pppl.gov>